RPC hodoscope to study inclined muons in Auger

Paulo Ferreira for the MARTA team

LIP Minho

Introduction

Resistive Plate Chambers (RPC) are detectors which are particularly suited and used in particle-physics experiments, indoors and outdoors [1]. These detectors have been used in the MARTA project with the aim of measuring ultra-high energy cosmic-ray showers [2, 3].

Two RPCs have been used by the MARTA team in a hodoscope for muon path tracking. The analysis that follows was performed to study the response of a Water Cherenkov Detector (WCD) to inclined muons. An analysis to the RPCs behaviour is necessary to understand the signal rate.

By using the previously established relations between the detector reduced electric field and its efficiency [4], coupled with the monitoring and interpretation of additional parameters, we were able to estimate the efficiency of the RPC and to relate them with the measured background and signal rates.

Experimental Setup

The hodoscope was composed with a RPC above the tank (top RPC) and one, inclined, at the side (bottom RPC). The data was collected between 30th November 2016 and 15th January 2017.

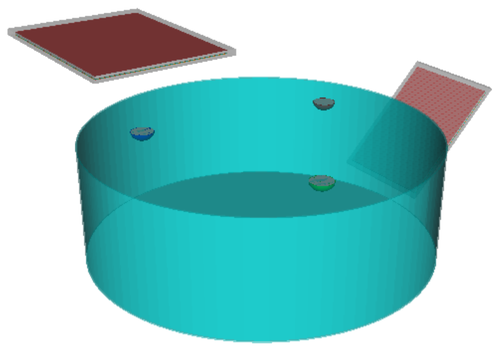

Figure 1: Three-dimensional representation of the experimental setup configuration for the inclined muons analysis.

Data Monitoring

From the RPCs we can access to:

- Background rates: obtained by counting the number of hits in a pad over 10 seconds. (Figure 2).
- Monitoring parameters: current I [nA], applied voltage HV [V], pressure P [mbar], relative humidity [%] and temperature T [°C], stored each minute (Figure 3).

The plots only show a week of acquisition to highlight the daily variations.

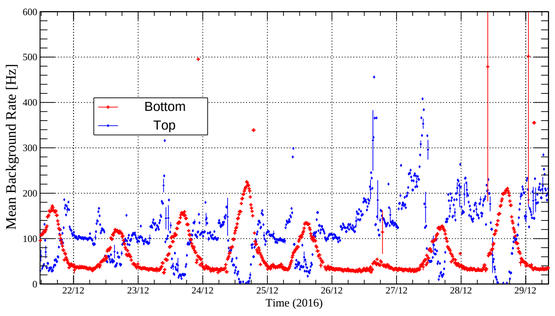

Figure 2: Mean values for the background rates of the top and bottom RPCs.

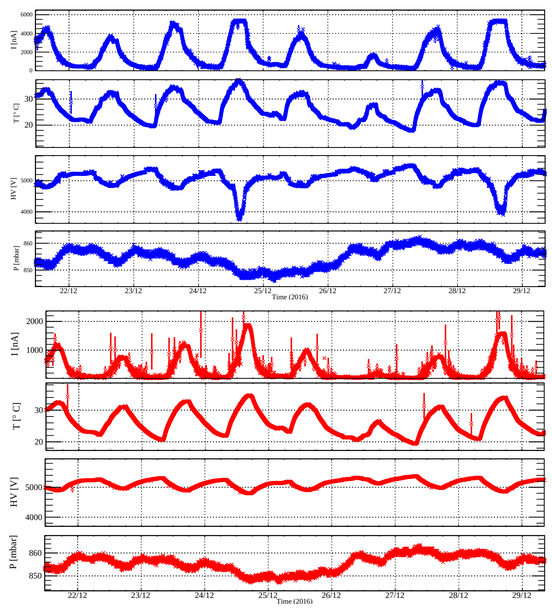

Figure 3: Variation of the monitored parameters of the top (up) and bottom (down) RPC as a function of time. From the upper to the lower picture: current, temperature, applied voltage and pressure.

Reduced Electric Field

The reduced electric field (E/N) in the RPCs is given by: [4, 5]

$$\frac{E}{N} = \frac{\kappa \times T_K}{d \times P} \times \left(HV - (\rho(T) \times t \times l) \cdot \frac{I}{A_{RPC}} \right) \quad (1)$$

Where T, I, P and HV are monitored parameters, $\kappa \sim 0.0138$ K^{-1} mbar cm^3 and l, d, t and A_{RPC} are geometric parameters of the RPCs. It is correlated with the efficiency as shown in [4].

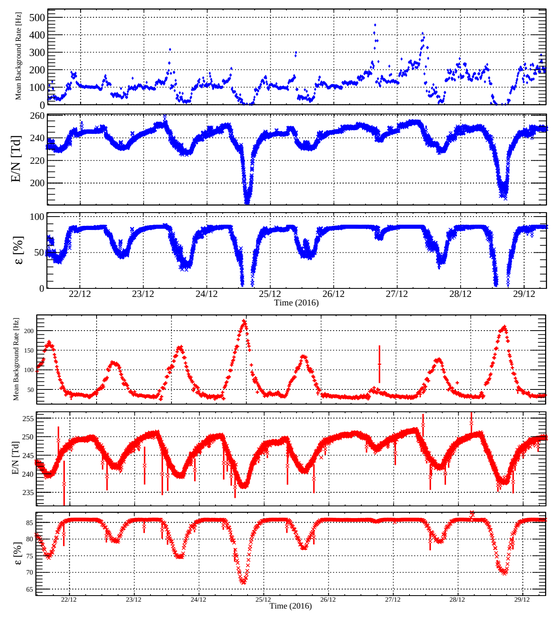

Figure 4: Comparison of the time variation of the mean background rate, the reduced electric field and the efficiency on the top (up) and bottom (down) RPCs.

The bottom RPC has a more stable and higher efficiency values, nearly always above 70%, while the top one drops often below 50%. A detailed analysis of E/N can explain this situation.

The effect of the current

Equation 1 can be divided in two different contributions for E/N: one for the applied voltage and a negative contribution from the current. Let them be respectively defined as $(E/N)'$ and $(E/N)''$, such that $E/N = (E/N)' - (E/N)''$, where:

$$\left(\frac{E}{N}\right)' = \frac{\kappa \times T_K}{d \times P} \times HV, \quad (2)$$

$$\left(\frac{E}{N}\right)'' = \frac{\kappa \times T_K}{d \times P} \times (\rho(T) \times t \times l) \cdot \frac{I}{A_{RPC}}. \quad (3)$$

The temperature and the pressure will influence both contributions. Therefore, the applied voltage and the current will settle the final E/N.

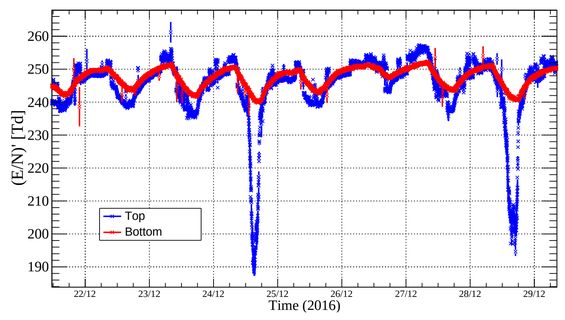

Figure 5: Variation $(E/N)'$ as a function of time for RPC top (blue) and bottom (red)

Although not constant, $(E/N)'$ is always high enough such that the RPCs have a high efficiency. However, in the top RPC, the values drop to the point where just a few less Td imply a huge decrease in the efficiency. Which is what happens to the total (E/N), when having in account the $(E/N)''$.

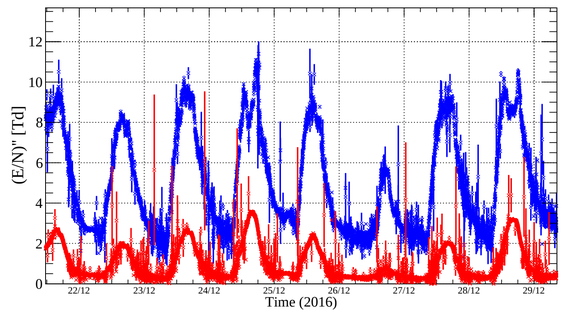

Figure 6: Variation $(E/N)''$ as a function of time for both RPCs.

To understand why $(E/N)''$ is higher in the top RPC we have to look at the current and the temperature in detail.

The increase of the background rates follows the increase of temperature, except when the top RPC loses its efficiency.

The temperature will increase the background rate (f_{back}) but also charge generated per ionization, Q_{ion}, which implies an increase of the current. The current I can be expressed as:

$$I(T) = f_{\mathrm{back}}(T) \times Q_{\mathrm{ion}}(T). \quad (4)$$

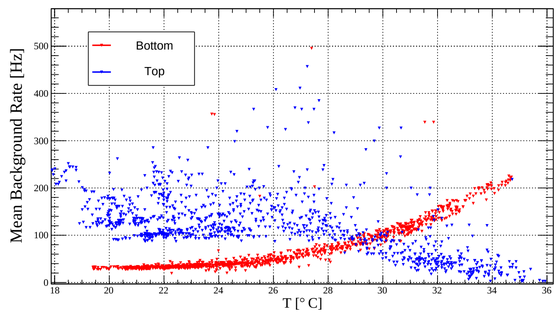

Figure 7: Relation between the temperature and the mean background rates for both RPCs.

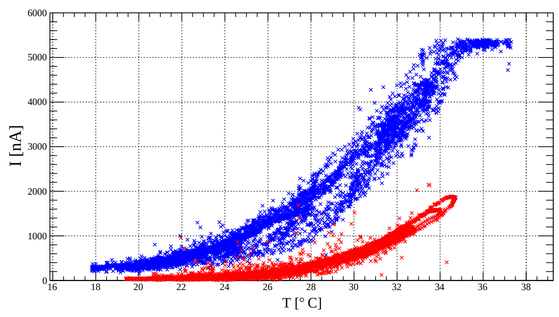

Figure 8: Relation between the temperature and the current values for RPC top (blue) and bottom (red).

This means that an increase of the temperature, since it increases both f_{back} and Q_{ion}, will produce an increase of the current. The same is valid for the bottom RPC, but the values of the background rate are always lower, in comparison to the top RPC (see Figure 8). Then, follows that $(E/N)''$ is higher on the top RPC, resulting in a lower (E/N) (see Figure 6).

Trigger Rates and Random Coincidences

Finally, the analysis can be completed by estimating the different rates: measured signal rate (after data selection, black dots), background rate from random coincidences (green dots) and estimated signal rate (red dots). The data selection is performed by crossing the RPCs and WCD data.

The estimated rate is determined from the atmospheric muon flux and the hodoscope efficiency, which is dependent on the geometry and the estimated RPCs efficiency.

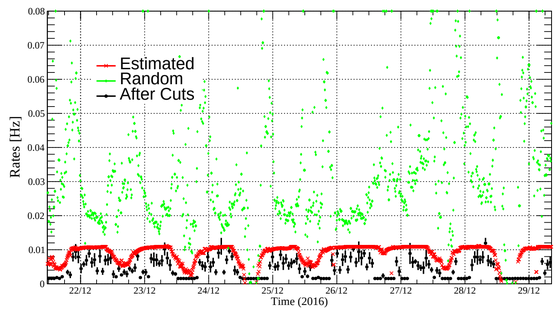

Figure 9: Estimated random coincidences rate (in green), estimated rate for muons (in red) and the rate after the data selection (in red) as a function of time.

Conclusions

By using precious analyses, we could show that the RPCs are operated in non optimized conditions and their behaviours can be understood with a constant monitoring. We could understand the RPCs signal rates in this geometric display, which is fundamental for the studies of the WCD response to inclined muons. A permanent monitoring is then necessary to guarantee the measurement of single muons.

References

[1] R. Santonica and R. Cardarelli, *Development of Resistive Plate Chambers*, *Nucl. Instrum. Metho.* **187** (1981) 377.

[2] L. Lopes, P. Fonte, and M. Pimenta, *Study of standalone RPC detectors for cosmic ray experiments in outdoor environment*, *JINST* **8** (2013) T03004.

[3] L. Lopes et al, *Resistive Plate Chambers for the Pierre Auger array upgrade*, *JINST* **9** (2014) C10023.

[4] L. Lopes et al, *Outdoor Field Experience with Autonomous RPC Based Stations*, *JINST* **11** (2016) C09011.

[5] R. Conceicao et al, *Autonomous RPCs for a Cosmic Ray ground array*, Proc. 35th ICRC (2017).

[6] P. Abreu et al, *MARTA: A high-energy cosmic-ray detector concept with high-accuracy muon measurement*, arXiv:1712.07685 (2017)

Acknowledgements

A special thanks to the MARTA team and to LIP for the contributions made to this analysis.